Observation of Shell Structures with Ions Stored in Traps*

J.J. Bollinger, S.L. Gilbert, and D.J. Wineland
Time and Frequency Division
National Institute of Standards and Technology
(formerly the National Bureau of Standards)
Boulder, CO 80303

ABSTRACT

We briefly discuss the possibility of using ions stored in traps to experimentally test the predictions of the one-component plasma (OCP) theory. We then report the observation of shell structures, a predicted feature of the finite OCP, with Be^+ ions stored in a Penning trap. Clouds containing up to 15 000 ions (density $\simeq 10^8$ cm^{-3}) were laser-cooled to temperatures of about 10 mK. Under these conditions, the ions are strongly coupled and exhibit liquidlike and solidlike behavior through the formation of concentric shells. The shells were observed by direct imaging of the laser-induced ion fluorescence for values of the Coulomb coupling constant Γ ranging from about 20 to 200.

Ions stored in traps can be approximated as a one-component plasma (OCP). An OCP consists of a single species of charge embedded in a uniform density background of opposite charge.[1] For the system of ions in a trap, the trapping fields play the role of the neutralizing background charge.[2] The thermodynamic properties of the OCP do not depend on the density and temperature separately, but only on the dimensionless coupling parameter $\Gamma = q^2/(a_s k_B T)$ which is a measure of the nearest neighbor potential energy divided by the thermal energy of a particle. The quantities q and T are the ion charge and temperature. The Wigner-Seitz radius a_s is defined by $4\pi a_s^3 n_0/3 = 1$, where $-qn_0$ is the charge density of the neutralizing background. An infinite OCP is predicted to exhibit liquidlike behavior (short-range order) for $\Gamma > 2$ and have a liquid-solid phase transition to a bcc lattice at $\Gamma = 178$.[3] Examples of strongly coupled OCP's can be found in dense astrophysical objects, for example, in the outer crust of a neutron star.[1] A current challenge to the experimentalist is to create a strongly coupled OCP in the laboratory and test the theoretical predictions for the infinite OCP. This would therefore provide information on very dense states of matter.

With the use of laser cooling, strongly coupled ions have been obtained at low ion densities in both the Penning and rf (Paul) traps.[4-7] The rf trap uses a quadrupole radio frequency field to confine ions to a region near the center of the trap.[8] A pseudopotential can be associated with the confining force of the rf trap; this pseudopotential describes the motion of a single ion in the trap for times long compared to the period of the rf frequency applied to the trap. This slow motion of an ion in an rf trap is known as the secular motion.[8] It is the analogue of the betatron motion of an ion in a storage ring. A fast micromotion at the rf trap frequency is superimposed on the slow secular motion of an ion. It is easy to show that ions in an rf trap behave like an OCP as long as the micromotion can be neglected relative to the secular motion of the ions.[2]

The rf micromotion, however, has important effects on ions stored in an rf trap. For example, the ion space charge electric fields can couple the energy of the micromotion into the secular motion. This process, known as rf heating,[8] has up to now, limited the number of stored ions that can be laser-cooled in an rf trap to approximately 100. In addition, the rf heating is

very nonlinear. It is greater in the disordered state of the stored ions than the ordered, crystallike state. If the cooling power is large enough to overcome the rf heating and some order starts to occur, the rf heating decreases and the ion temperature rapidly decreases resulting in a cold, ordered state.[10,11] In essence, the ion cloud has two states, a hot disordered state and a cold, ordered state.[10,11] This may make it difficult to control the ion temperature and study the onset of order. If the difficulties in laser cooling many ions and in controlling the ion temperature can be overcome, it should be possible to use ions in an rf trap to experimentally test the predictions of the infinite, strongly coupled OCP. Similar considerations may apply with ions in a storage ring.

These problems do not occur for ions stored in a Penning trap because only static electric and magnetic fields are used for confinement. Consequently, it has so far been possible to laser-cool larger numbers of ions in a Penning trap. We have been able to laser-cool up to 10^5 Be^+ ions in a Penning trap to temperatures less than 1 K. A currently unanswered question is how many stored ions are required for infinite volume behavior, i.e. the appearance of a bcc lattice for $\Gamma > 178$. For a finite plasma consisting of a hundred to a few thousand ions, the boundary conditions are predicted to have a significant effect on the plasma state. Simulations involving these numbers of ions in a spherical trap potential predict that the ion cloud will separate into concentric spherical shells.[12-14] Instead of a sharp phase transition, the system is expected to evolve gradually from a liquid state characterized by short-range order and diffusion in all directions, to a state where there is diffusion within a shell but no diffusion between the shells (liquid within a shell, solidlike in the radial direction), and ultimately to an overall solidlike state.[14] These conclusions should apply to a nonspherical trap potential as well if the spherical shells are replaced with shells approximating spheroids. Preliminary independent investigations[15,16] of the nonspherical case support this conjecture.

We have observed shell structures with $^9Be^+$ ions stored in a Penning trap. These observations were first reported in Ref. 7, and the description of the experiment and observation are repeated below. The $^9Be^+$ ions were trapped in the cylindrical Penning trap shown schematically in Fig. 1. A

magnetic field $\vec{B} = B\hat{z}$ ($B = 1.92$ T) produced by a superconducting magnet confined the ions in the direction perpendicular to the z axis. A static potential V_0 between the end and central cylinders confined the ions in the z direction to a region near the center of the trap. The dimensions of the trap electrodes were chosen so that the first anharmonic term in the expansion of the trapping potential was zero. Over the region near the trap center, the potential can be expressed (in cylindrical coordinates) as $\Phi \simeq AV_0(2z^2-r^2)$ where $A = 0.146\ cm^{-2}$. A background pressure of 10^{-8} Pa ($\approx 10^{-10}$ Torr) was maintained by a triode sputter-ion pump. The stored ions can be characterized by a thermal distribution where the "parallel" (to the z axis) temperature $T_\parallel$ is approximately equal to the "perpendicular" temperature $T_\perp$ (from the cyclotron motion). This thermal distribution is superimposed on a uniform rotation of the cloud[2,4] at frequency ω which, at the low temperatures of this experiment, is due to the $\vec{E}\times\vec{B}$ drift, where $\vec{E}$ is the electric field due to the trap voltage and the space charge of the ions.

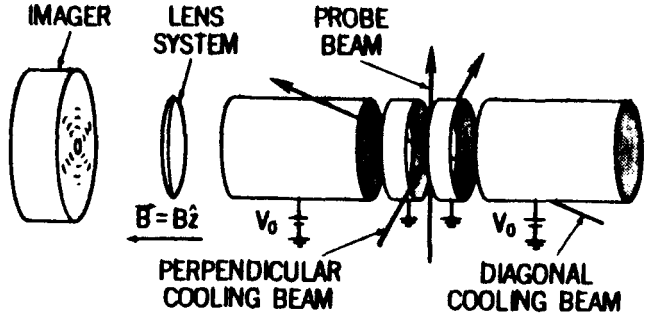

Fig. 1. Schematic drawing of the trap electrodes, laser beams, and imaging system (not to scale). The overall length of the trap is 10.2 cm. The trap consists of two end cylinders and two electrically connected central cylinders with 2.5 cm inner diameters. Ion clouds are typically less than 1 mm in both diameter and axial length. The diagonal cooling beam crosses the cloud at an angle of 51° with respect to the z axis.

The ions were laser cooled and optically pumped into the $2s\ ^2S_{\frac{1}{2}}(M_I=3/2, M_J=1/2)$ state by driving the $2s\ ^2S_{\frac{1}{2}}(3/2,1/2) \rightarrow 2p\ ^2P_{3/2}(3/2,3/2)$ transition slightly below its resonant frequency.[4] The 313-nm cooling radiation ($\approx 30\ \mu W$) could be directed perpendicularly to the magnetic field and/or along a diagonal as indicated in Fig. 1. In addition to cooling the ions, the laser also applied an overall torque which could either compress or expand the cloud.[4] This allowed us to control the cloud size by choosing the

radial positions (and thus the torques) of the perpendicular and diagonal beams.

About 0.04% of the 313-nm fluorescence from the decay of the $^2P_{3/2}$ state was focused by f/10 optics onto the photocathode of a resistive-anode photon-counting imaging tube. The imager was located along the z axis, about 1 m from the ions. The imaging optics was composed of a three-stage lens system with overall magnification of 27 and a resolution (FWHM) of about 5 μm (specifically, the image of a point source when referred to the position of the ions was approximately 5 μm in diameter). Counting rates ranged from 2 to 15 kHz. Positions of the photons arriving at the imager were displayed in real time on an oscilloscope while being integrated by a computer.

A second laser (power $\approx$ 1 μW, beam waist $\approx$ 30 μm) was used to map the shell structure of the cloud. This probe laser was tuned to the same transition as the cooling laser and was directed through the cloud perpendicularly to the magnetic field. With the probe laser turned on continuously, the cooling laser could be chopped at 2 kHz (50% duty cycle) and the image signal integrated only when the cooling laser was off. Different portions of the cloud could be imaged by the translation of the probe beam, in a calibrated fashion, either parallel or perpendicular to the z axis. Images were also obtained from the ion fluorescence of all three laser beams.

The probe beam was also used to measure the cloud rotation frequency ω and ion temperature.[4] For these measurements, the probe laser was tuned to the 2s $^2S_{\frac{1}{2}}(3/2,1/2) \rightarrow$ 2p $^2P_{3/2}(3/2,-1/2)$ "depopulation" transition. Ions in the 2p $^2P_{3/2}(3/2,-1/2)$ state can decay to the 2s $^2S_{\frac{1}{2}}(3/2,-1/2)$ state, temporarily removing some of the ion population from the 2s $^2S_{\frac{1}{2}}(3/2,1/2)$ state. This results in a decrease in the cooling fluorescence as the probe laser is scanned through the depopulation transition. We determined ω by measuring the change in the Doppler shift of the depopulation signal as the probe beam was translated perpendicularly to the z axis. The density n_0 could then be calculated[2,4] from $n_0 = m\omega(\Omega-\omega)/2\pi q^2$, where $\Omega = qB/mc$ is the cyclotron frequency. With use of n_0 and the cloud size obtained from probe-beam images, the total number of ions was calculated. The ion temperature was derived from the Doppler broadening contribution to the width of the depopulation signal.[4]

The temperature $T_\perp$ was measured with probe beam perpendicular to the magnetic field and $T_\parallel$ was measured with the probe beam parallel to the magnetic field direction (not shown in Fig. 1). In the latter case, crossed polarizers were used to reduce the intensity of the probe beam at the imager. From the measured values of the temperature T and the density n_0, Γ was calculated with Eq. (1). In the case where $T_\perp \neq T_\parallel$, the larger temperature was used in the calculation of Γ.

We have observed shell structure in clouds containing as few as 20 ions (one shell) and as many as 15 000 ions (sixteen shells). Images covering this range are shown in Fig. 2. Even with 15 000 ions in the trap there is no evidence for infinite volume behavior. We measured the coupling constant Γ for several clouds containing about 1000 ions. Drift in the system parameters was checked by verifying that the same images were obtained before and after the cloud rotation frequency and ion temperatures were measured. Figure 3 shows examples of shell structures at two different values of Γ. The first image is an example of high coupling ($\Gamma \approx 180$) and shows very good shell definition in an intensity plot across the cloud. The second image is an example of lower coupling ($\Gamma \approx 50$) and was obtained with cooling only perpendicular to the magnetic field. Variations in peak intensities equidistant from the z axis are due to signal-to-noise limitations and imperfect alignment between the imager x axis and the probe beam.

We obtained three-dimensional information on the shell structure by taking probe images at different z positions; two types of shell structure were present under different circumstances. The first type showed shell curvature near the ends of the cloud, indicating that the shells may have been closed spheroids. Shell closure was difficult to verify because of a lack of sharp images near the ends of the cloud where the curvature was greatest. This may have been due to the averaging of the shells over the axial width of the probe beam. In the other type of shell structure, it was clear that the shells were concentric right circular cylinders with progressively longer cylinders near the center. An example of these data is shown in Fig. 4. Other evidence for cylindrical shells was obtained from the observation that shells in the diagonal-beam images occurred at the same cylindrical radii as those from the perpendicular beams. This can be seen in

the three-beam images such as that shown in Fig. 2(c). Systematic causes of these two different shell configurations have not yet been identified.

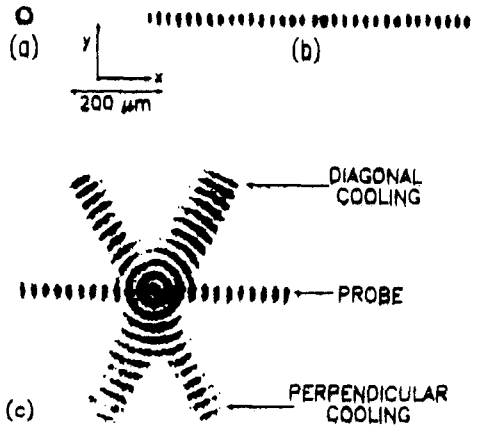

Fig. 2. Images of shell structures. (a) A single shell in a cloud containing approximately 20 ions. Trap voltage V_0 = 14 V and cloud aspect ratio a_r (axial length/diameter) ≈ 6.5. This image was obtained from the ion fluorescence of the perpendicular and diagonal cooling beams. (b) Sixteen shells (probe-beam ion fluorescence only) in a cloud containing about 15 000 ions with V_0 = 100 V and a_r ≈ 0.8. (c) Eleven shells plus a center column in the same cloud as (b), with V_0 = 28 V and a_r ≈ 2.4. This image shows the ion fluorescence from all three laser beams. Integration times were about 100 s for all images.

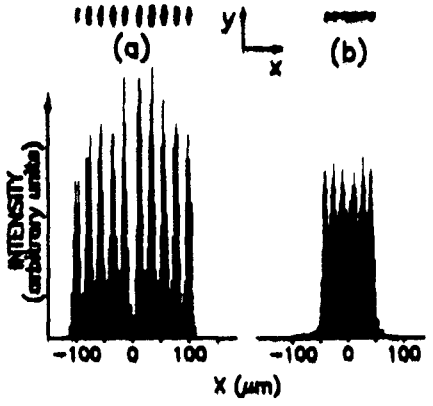

Fig. 3. Intensity plots along the imager x axis (parallel to the probe beam) through the center of the ion cloud with corresponding images (above). (a) $\Gamma = 180^{+90}_{-70}$ ($T = 6\ ^{+4}_{-2}$ mK, $n_0 \approx 7\times10^7$ ions cm^{-3}). Cloud aspect ratio $a_r \approx 3.5$. (b) $\Gamma = 50^{+30}_{-20}$ ($T = 33^{+17}_{-13}$ mK, $n_0 = 2\times10^8$ ions cm^{-3}), $a_r \approx 5$. The clouds contained about 1000 ions in both cases.

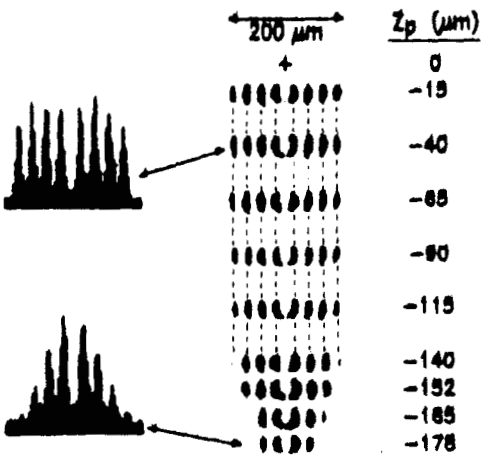

Fig. 4. Data showing evidence for concentric cylindrical shells. On the right is a series of images obtained with the probe beam for different z positions z_p of the probe beam (lower half of the cloud only). Intensity plots for z_p = -40 μm and z_p = -178 μm are shown on the left. The cloud aspect ratio a_r was about 1.9.

One comparison which can be made between the theoretical calculations and our experimental results is the relationship between the number of shells and the number of ions, N_i, in a cloud. For a spherical cloud, approximately $(N_i/4)^{1/3}$ shells are predicted.[12] For the nearly spherical cloud of Fig. 2(b) ($N_i \simeq 15\,000$), this formula predicts 15.5 shells and we measure 16. At present, it is difficult to make further quantitative comparisons between our data and the theoretical calculations. For example, there is substantial uncertainty in our measurement of Γ due to uncertainty in the temperature measurement. Our data do agree qualitatively with the simulations with the exception, in some cases, of the presence of an open-cylinder shell structure as opposed to the predicted closed spheroids. Schiffer has suggested[15] that shear (that is, different rotation frequencies) between the shells may account for this discrepancy. In our experiment, shear could be caused by differential laser torque or the presence of impurity ions.[17] For the data here, we have determined that the rotation frequency does not vary by more than 30% across the cloud. This is comparable to the limits discussed in Refs. 17 and 18.

Future improvements will allow a more complete comparison of the data and the simulations, such as the relationship between shell definition and Γ for a

variety of conditions. Also, we have observed that it is possible, using the probe depopulation transition, to tag ions in different parts of the cloud and see the presence (or lack) of ion diffusion. In preliminary measurements we have observed states where the diffusion between shells is slow compared to the diffusion within a shell, as well as near solidlike states where the diffusion both between shells and within a shell is slow. Finally, with more laser power, even larger clouds (10^5 ions or more) can be cooled to these temperatures (10 mK). This may permit observation, by Bragg scattering,[4] of the predicted infinite volume structure.

We gratefully acknowledge the support of the U.S. Office of Naval Research and the Air Force Office of Scientific Research. We thank Wayne M. Itano and Carl Weimer for carefully reading the manuscript.

1. S. Ichimaru, H. Iyetomi, and S. Tanaka, Phys. Rep. 149, 91 (1987), and references therein.
2. J.H. Malmberg and T.M. O'Neil, Phys. Rev. Lett. 39, 1333 (1977); D.J. Wineland, J.J. Bollinger, W.M. Itano, and J.D. Prestage, J. Opt. Soc. Am. B2, 1721 (1985); D.J. Wineland et al., in Non-Neutral Plasma Physics, edited by C.W. Roberson and C.F. Driscoll (American Institute of Physics, New York, 1988) p. 93.
3. E. Pollack and J. Hansen, Phys. Rev. A8, 3110 (1973); W.L. Slatterly, G.D. Doolen, and H.E. DeWitt, ibid 21, 2087 (1980); 26, 2255 (1982).
4. J.J. Bollinger and D.J. Wineland, Phys. Rev. Lett. 53, 348 (1984); L.R. Brewer, J.D. Prestage, J.J. Bollinger, and D.J. Wineland, in Strongly Coupled Plasma Physics, edited by F.J. Rogers and H.E. DeWitt (Plenum, New York, 1987), p. 19.
5. F. Diedrich, E. Peik, J.M. Chen, W. Quint, and H. Walter, Phys. Rev. Lett. 59, 2931 (1987).
6. D.J. Wineland, J.C. Bergquist, W.M. Itano, J.J. Bollinger, and C.H. Manney, Phys. Rev. Lett. 59, 2935 (1987).
7. S.L. Gilbert, J.J. Bollinger, and D.J. Wineland, Phys. Rev. Lett. 60, 2022 (1988).
8. D.J. Wineland, W.M. Itano, and R.S. Van Dyck, Jr., Adv. At. Mol. Phys. 19, 135 (1983) and references therein.

9. D.A. Church and H.G. Dehmelt, J. Appl. Phys. 40, 3421 (1969); H.G. Dehmelt, in Advances in Laser Spectroscopy, edited by F.T. Arecchi, F. Strumia, and H. Walter (Plenum, New York, 1983) p. 153.
10. J. Hoffnagle, R.G. Devoe, L. Reyna, and R.G. Brewer, Phys. Rev. Lett. 61, 255 (1988).
11. R. Blümel et al., Nature 334, 309 (1988).
12. A. Rahman and J.P. Schiffer, Phys. Rev. Lett. 57, 1133 (1986); J.P. Schiffer, Phys. Rev. Lett. 61, 1843 (1988).
13. H. Totsuju, in Strongly Coupled Plasma Physics, edited by F.J. Rogers and H.E. DeWitt (Plenum, New York, 1987), p. 19.
14. D.H.E. Dubin and T.M. O'Neil, Phys. Rev. Lett. 60, 511 (1988).
15. J.P. Schiffer, Argonne Natl. Lab., Argonne, IL, private communication.
16. D.H.E. Dubin, Dept. of Phys., UCSD, La Jolla, CA, private communication.
17. D.J. Larson, J.C. Bergquist, J.J. Bollinger, W.M. Itano, and D.J. Wineland, Phys. Rev. Lett. 57, 70 (1986).
18. L.R. Brewer, J.D. Prestage, J.J. Bollinger, W.M. Itano, D.J. Larson, and D.J. Wineland, Phys. Rev. A38, 859 (1988).